Submonolayer Magnetism of Fe(110) on W(110): Finite Width Scaling of Stripes and Percolation between Islands

H. J. Elmers, J. Hauschild, H. Höche,* and U. Gradmann

Physikalisches Institut, Technische Universität Clausthal, D38678 Clausthal-Zellerfeld, Germany

H. Bethge, D. Heuer, and U. Köhler

Institut für Festkörperphysik, Universität Hannover, D30167 Hannover, Germany

Relations between magnetism and morphology in submonolayer films of Fe(110) on W(110) were studied using spin polarized electron diffraction and scanning tunneling microscopy. Films prepared at 600 K form monolayer stripes along with the W steps; they are ferromagnetic with T_c slowly decreasing from 225 K near $\theta = 1$ to 180 K near $\theta = 0.1$. The decrease scales with $1/\theta$. Films prepared at 300 K nucleate by islands which start to coalesce near $\theta = 0.6$. For $\theta \leq 0.58$, they are superparamagnetic at $T \geq 115$ K. In a narrow θ range of only 2%, magnetic percolation occurs, resulting in ferromagnetism with $T_c \geq 190$ K for $\theta \geq 0.60$.

In 3D ferromagnets, primary magnetic properties like Curie temperature, spontaneous magnetization, and its temperature dependence depend only weakly on structural defects. In thin films, in particular in ultrathin films down to the monolayer, they become structural sensitive properties [1]. This shows up in a delicate dependence on the preparation conditions. Scanning tunneling microscopy (STM) offers a powerful access to the nanomorphology of ultrathin epitaxial films as a basis for a thorough understanding of their magnetic properties. Accordingly, STM studies have been preformed recently for ultrathin films of fcc γ-Fe on Cu(111) [2], Co on Cu(111) [3], Co on Cu(100) [4], and γ-Fe on Cu(100) [5–8]. Co on Cu, in the monolayer regime, forms complicated interdiffusion structures, and γ-Fe on Cu is one of the most complicated metastable systems at all. A study which directly compares magnetic properties with morphology from STM has not yet been published, to our knowledge. In this Letter, we present a first study of this type, for submonolayers of Fe(110) on W(110). Fe(110) films on W(110) are unique in that they start growing by a stable monolayer [9], pseudomorphic with the W substrate. Accordingly, the pseudomophic monolayer Fe(110) on W(110) is the only example for which true monolayer ferromagnetism could be studied experimentally, both by conversion electron Mössbauer spectroscopy (CEMS) [10–12] and by magnetometry [13]. Extending these studies now to the submonolayer regime, we analyze well defined structures, given by a literally 2D system of Fe atoms, all sitting in one atomic plane, in lateral positions determined by the W substrate. We focus on the influence of this 2D atomic distribution on ferromagnetic properties. Submonolayer magnetism has been addressed previously by Dürr et al. [14], who suggested that detailed analysis of submonolayer magnetism could provide insight in 2D percolation phenomena. This insight in 2D magnetic percolation will be given for our Fe(110) films prepared at

RT, whereas films prepared at 660 K are ferromagnetic down to 0.05 monolayer.

We started from an observation in Ag-covered Fe(110) monolayers on W(110) [11], for which T_c was independent of the coverage θ, for $0.5 < \theta < 1.0$, when the films were prepared at 500 K, whereas T_c decreased monotonously with θ for films prepared at 300 K. This was tentatively explained by step-flow growth of Fe stripes from W steps at 500 K, contrary to growth by islands at 300 K, an idea which was on principle confirmed by low energy electron diffraction (LEED) [15]. A full confirmation and detailed insight in the submonolayer morphology will be given in the following using STM. For magnetic analysis we use spin polarized low energy electron diffraction (SPLEED), performed in a separate UHV system. In both systems, Fe was grown on similarly prepared atomically clean and smooth W(110) surfaces, at pressures below 10^{-10} Torr. Because of the mosaic spread of the substrate, atomic steps with varying distances of some 10 nm and different orientations were present in the substrates. All submonolayer films showed the sharp LEED pattern of the W substrate, that means that they were pseudomorphic with W, strained in the plane by the misfit of 9.4%. Monolayer coverage θ was measured in the SPLEED system with an accuracy of 2% using a quartz oscillator balance. In the STM system, thickness was determined by directly counting θ in the images. All films of this study were uncovered. This makes an essential difference to the previous CEMS study on Ag-covered submonolayers [11], because the Ag coverage changes T_c strongly [10,16] and indirect coupling through the Ag coverage may be important.

The growth mode of films prepared at 300 K is visualized by the STM images of Fig. 1. As seen in Fig. 1(a), the films start growing by islands [upper level (Fe) bright] both on the W terraces [lower level (W) dark] and at the steps of the substrate, with some dendritic tendencies. Note the
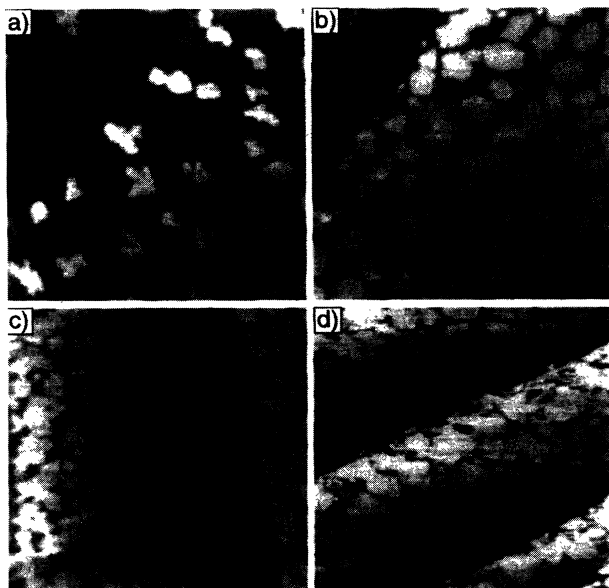
FIG. 1. STM images of Fe(110) films, prepared at RT on W(110), all 70 nm × 70 nm in size, with [001] horizontal. (a) $\theta = 0.23$; (b) $\theta = 0.53$; (c) $\theta = 0.66$; (d) $\theta = 0.85$. Upper levels (Fe) bright; lower levels (W) dark.

FIG. 2. Partial coverage $\theta_{(A>A_0)}$ by islands of area $A > A_0$, vs A_0, for the films of Fig. 1, prepared at RT. Each symbol represents one island; note the transition from many small islands for thin films to few large islands for thick films.

decoration of the initially straight W steps by Fe dendrites. With further growth, the island size increases and the dendritic shape is smoothened [Fig. 1(b)], but for $\theta < 0.6$ the islands remain still separated by channels. Apparently there is some inhibition of coalescence, presumably caused by the misfit. Only above $\theta = 0.6$, coalescence starts by narrow bridges between the islands. This is shown in Fig. 1(c) for $\theta = 0.66$, where we observe just a spacious net of percolation paths, with some isolated islands still between. With further growth [Fig. 1(d)], coalescence proceeds, but channels and even some small islands remain up to $\theta = 0.8$. In order to obtain a more quantitative insight in the coalescence process, we determined, by counting islands of different area A, the partial coverage $\theta_{(A>A_0)}$ of the surface by islands of an area $A > A_0$, as a function of A_0. This is shown in Fig. 2 for the samples of Figs. 1(a)–1(d). Whereas the thinner samples ($\theta = \theta_{(A>A_0)} = 0.23$, 0.53) consist completely of islands with $A < 150$ nm^2, the coalescence near $\theta = 0.6$ shows up in a steep increase of the partial coverage by coalesced large islands ($A > 150$ nm^2); however, a considerable fraction of "small," typically non-coalesced islands is left, contributing roughly $\frac{1}{3}$ of the total Fe coverage even at $\theta = 0.66$. The coalescence from a system of small islands to a system of large coalesced islands is smooth.

The growth mode is completely different at elevated temperatures, see Figs. 3(a) and 3(b). We observe step-flow growth from the steps of the substrate, with continuous Fe stripes from the very lowest coverages on [Fig. 3(a)], and some sawtoothlike roughening at intermediate coverages [Fig. 3(b)]. However, continuous stripes along the substrate steps are formed in all stages. The transition between a W level and its Fe continuation is
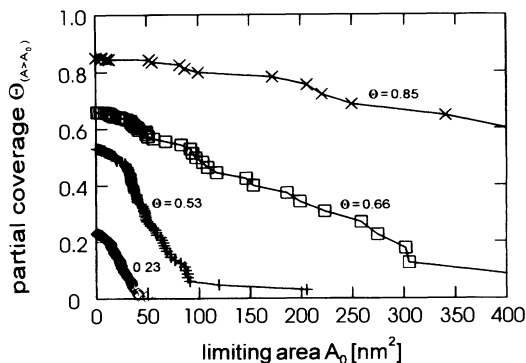
represented by faint lines only, indicated by arrows. Images not shown in Fig. 3 confirm that the second layer starts only after completion of the first one. Apparently, a film with $\theta = 1$, prepared at $T \geq 570$ K, would provide a nearly perfect monolayer, the only defects being given by the steps in the substrate.

SPLEED was performed using transversally polarized electrons from a GaAs source irradiated by circularly polarized light. We measured the different electron reflectivities I^+ and I^-, for the electron spin moment parallel or antiparallel to the film magnetization, respectively. As a measure of the film magnetic moment, we used the exchange asymmetry $A_{ex} = (I^+ - I^-)/(I^+ + I^-)$. For the choice of the reflection geometry, we started from the fact that the monolayer is magnetized along $[1\bar{1}0]$, as a result of a strong uniaxial surface type in-plane anisotropy of the order of 0.6 mJ/m^2 [9]. Accordingly, we measured A_{ex}, in the specular elastic beam, in the $(1\bar{1}0)$ scattering plane, the scattering normal $[1\bar{1}0]$ coinciding with the quantization axis of electron spin ($E = 49$ eV, reflection angle 32°). For these scattering conditions, A_{ex} is maximum with respect to both energy and scattering angle, independent of the temperature. Under these conditions it can be expected that A_{ex} is proportional to the (remanent) magnetization, for varying temperatures, at least near T_c. In a standard run, the sample was cooled down to 115 K in an external
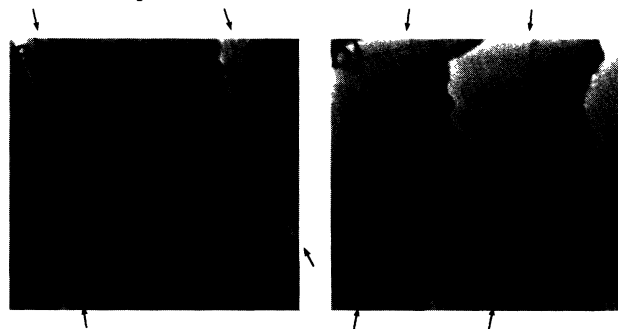

FIG. 3. As Fig. 1, but for films prepared at 570 K. (a) $\theta = 0.14$; (b) $\theta = 0.52$. The strong contrast marks the edge of the Fe layer; the faint contrast (straight line, indicated by arrows) the transition from W to Fe at the same level, at W steps.
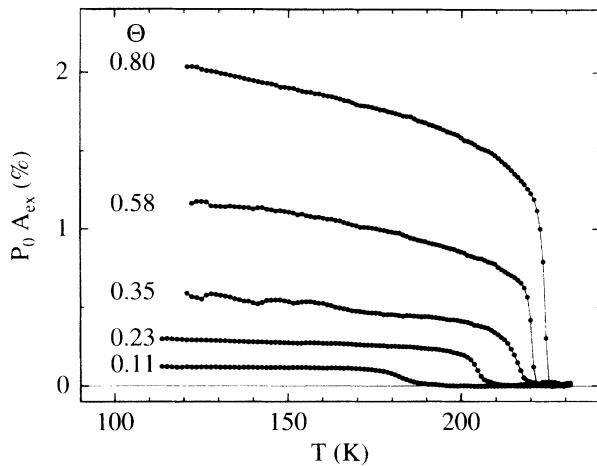
FIG. 4. $P_0 A_{ex}$ vs T for electron reflection from Fe(110) films prepared at 660 K on W(110); Fe coverage θ is given as a parameter. P_0 is the spin polarization of the incident electron beam, roughly 20%.

field of 200 G. A_{ex} was subsequently measured for slowly raising temperatures, in a residual field of 40 mG. Curves of A_{ex} vs T taken in this way are shown in Figs. 4 and 5 for films prepared at 660 and 300 K, respectively, with θ as a parameter. The same curves could be obtained for cooling down with periodic remagnetization in pulses of 200 G. This thermal reversibility indicates a saturated single-domain state of the films.

The magnetic behavior of films prepared at 660 K (Fig. 4) is reasonable. T_c increases monotonously with θ, and so does the maximum value $A_{ex,115\,K}$, as expected from a virtually constant magnetization in the magnetized stripes; see Figs. 3(a) and 3(b). We omit data for $\theta > 0.8$, because both A_{ex} and T_c were found to decrease with approach to the monolayer. Apparently, coupling between the stripes, which occurs with approach to $\theta = 1$, induces more complicated, inhomogeneous magnetization structures, which remain to be analyzed. On a microscopic
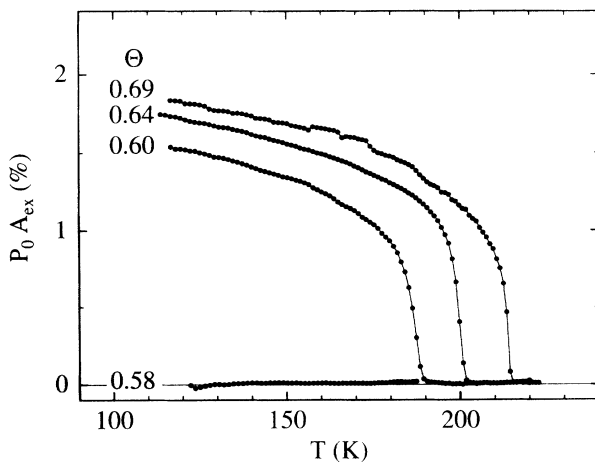
scale, coverage θ is the ratio between the width w of the Fe stripes and the width W of the W terraces, respectively, $w = \theta W$. We therefore virtually observe, with decreasing θ, the decrease of A_{ex} and of T_c with decreasing stripe width, that means the incipient transition from 2D to 1D magnetism. In other terms, we observe, for the first time, a finite width scaling of T_c in narrow stripes, quite analogous to the well-known finite thickness scaling of T_c in thin films, its decrease with decreasing thickness [17–19], which in turn can be interpreted as a transition from 3D to 2D magnetism. We plotted $T_c(\theta)$, operationally defined by the section of the tangent in the point of inflexion with the axis, as shown in Fig. 6. Following general ideas of finite size scaling [19,20], we fitted the data by a power law $[T_c(\text{ML}) - T_c(\theta)]/T_c(\text{ML}) = (\theta/\theta_0)^{-\lambda}$, resulting in $T_c(\text{ML}) = 230$ K, which we take as the Curie temperature of the uncovered extended monolayer, in rough agreement with previous estimates $[T_c(\text{ML}) = 210$ K $[10]]$. The fit further results in a "shift exponent" $\lambda = 1.03 \pm 0.14$, which should be connected with the critical exponent ν of the correlation length by $\lambda = 1/\nu$ [20]; our results, obtained from uniaxial monolayer stripes, are in accordance with the value $\nu = 1.0$ of the 2D Ising model. Finally, the fit results in $\theta_0 = 0.02$, corresponding to a stripe width $w_0 = W\theta_0$ for which the extrapolation of T_c disappears. The width W of the W terraces, being caused by the mosaic spread of the substrate, shows considerable dispersion, with a mean value which could only roughly be estimated to 40 nm, resulting in $w_0 = 0.8$ nm, corresponding to four atomic chains in the stripe, a rough estimate of the number of chains which are needed to obtain a ferromagnetic stripe at low temperatures. The curve for $\theta = 0.8$ in Fig. 4, which we consider as the best approximation to the extended monolayer, shows a remarkably steep transition, without the frequently observed tails above T_c. In a critical regime $0.004 < (T_c - T)/T_c < 0.05$, we deter-
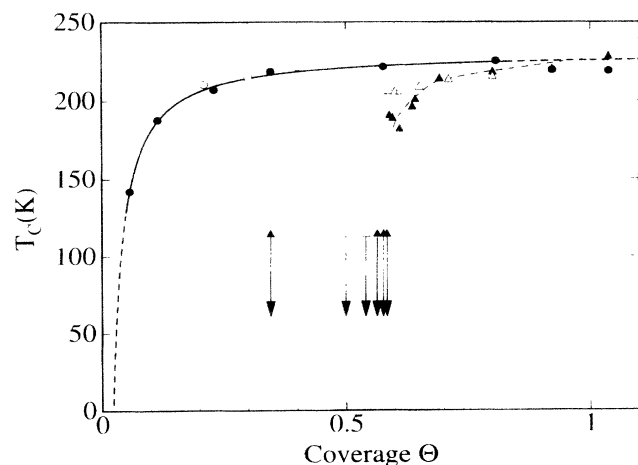

FIG. 5. $P_0 A_{ex}$ vs T for electron reflection from Fe(110) films prepared at RT on W(110); Fe coverage θ is given as a parameter.

FIG. 6. Curie temperature T_c vs coverage θ for Fe(110) prepared on W(110) at $T_p = 300$ K (▲), 390 K (△), 470 K (○), and 660 K (●), respectively. Full line, power law fit, for $T_p = 660$ K. Dashed line, guide to the eye for $T_p = 300$ K. Downward arrows indicate that $T_c < 115$ K (lower temperature limit).

mined a critical exponent $\beta = 0.123$, which nicely fits the value $\beta = \frac{1}{8}$ of the 2D Ising model.

The dependence of A_{ex} on θ and T is completely different for films prepared at RT; see Fig. 5. Whereas $A_{ex,115 K}/\theta$ is nearly constant for $\theta \geq 0.60$, A_{ex} then abruptly drops and completely disappears for $\theta \leq 0.58$, for all temperatures $T \geq 115$ K. The same steep drop of magnetic order was observed for films prepared at 390 K. Because the films for $\theta \leq 0.58$ consist of separated islands, the most obvious explanation for the absence of magnetic order in them is superparamagnetism. For a quantitative check, we ask for the blocking area at 115 K, below which single islands become superparamagnetic [21], to be calculated from the in-plane anisotropy of the monolayer, K_{sp}^{monol}, which has not been measured. A rough estimate, using the surface anisotropy of thick free Fe(110) films on W(110) (0.61 mJ/m^2) [22], and the observation that, for the case of the out-of-plane anisotropy of the Ag-covered monolayer, the monolayer anisotropy is 55% of the anisotropy of thick films [9], results in $K_{sp}^{monol} = 0.33$ mJ/m^2. This results in a blocking area of 130 nm^2. As seen in Fig. 2, the noncoalesced islands for $\theta \leq 0.53$ are all below this limit. This rough estimate thus confirms superparamagnetism as a reasonable explanation for the absence of magnetic order for $\theta \leq 0.58$. The most striking phenomenon is the steep rise in a narrow θ interval of only 2%, from a completely nonmagnetic state at $\theta = 0.58$ to a magnetic state at $\theta = 0.60$. Note that at this coverage not only T_c reaches nearly the extended monolayer value, but also A_{ex} reaches nearly the value which would be expected from Fig. 4 for this coverage. This means that virtually all components of the partial monolayer take part in this sudden transition from superparamagnetism at $\theta = 0.58$ to ferromagnetism at $\theta = 0.60$. In contrast, from Figs. 1 and 2 we estimate that at $\theta = 0.60$ at least half of the film still consists of islands with an area below the superparamagnetic limit of 130 nm^2. A soft coalescence process (see Figs. 1 and 2) results in an extremely sharp magnetic percolation, which we understand as the formation of long range exchange coupling paths. Obviously, this percolation occurs in a system not of single atoms but of previously superparamagnetic islands. The data suggest a process in which magnetic order starts from a loose net of coalesced islands, from which it spreads avalanchelike over the whole sample, including the considerable fraction of isolated islands: Percolation is triggered by the coalescence of superparamagnetic to thermally stable islands. Presumably, some indirect coupling via the W substrate is involved in this avalanche process, the details of which remain to be explained, hopefully from experiments with SPLEED and STM in one system.

In conclusion, we presented a comparative study of structure and magnetism for submonolayer Fe(110) films on W(110). Magnetic properties were detected by SPLEED, 2D morphology by STM. We observe a dramatic dependence on the preparation temperatures both for the growth modes and for the magnetic properties. Films prepared at 660 K form stripes along the W steps which are ferromagnetic down to a coverage $\theta = 0.05$. Finite width scaling of T_c in stripes has been observed for the first time; that means that T_c depends on the width of the stripes in a similar way as T_c in thin films depends on their thickness. Films prepared at RT are nonmagnetic at 115 K for $\theta \leq 0.58$. They become ferromagnetic over the very narrow range between $\theta = 0.58$ and 0.60, with a steep rise of T_c to 190 K at $\theta = 0.60$. This magnetic percolation is triggered by the coalescence of superparamagnetic to thermally stable islands. It seems to be assisted by indirect coupling via the substrate, as indicated by the avalanchelike spread of magnetic order over the whole sample.

[1] U. Gradmann, in Handbook of Magnetic Materials edited by K. H. J. Buschow (Elsevier, Amsterdam, 1993) Vol. 7/1, pp. 1–96.

[2] A. Brodde et al., Phys. Rev. B 47, 6609 (1993).

[3] J. d. la Figuera, J. E. Prieto, C. Ocal, and R. Miranda, Phys. Rev. B 47, 13 043 (1993).

[4] A. K. Schmid et al., Phys. Rev. B 48, 2855 (1993).

[5] D. D. Chambliss, R. J. Wilson, and S. Chiang, J. Vac. Sci. Technol. A 10, 1993 (1992).

[6] M. Wuttig et al., Surf. Sci. 291, 14 (1993).

[7] A. Brodde and H. Neddermeyer, Surf. Sci. 287, 988 (1993).

[8] J. Giergiel et al., Surf. Sci. 310, 1 (1994).

[9] U. Gradmann, M. Przybylski, H. J. Elmers, and G. Liu, Appl. Phys. A 49, 563 (1989).

[10] M. Przybylski and U. Gradmann, Phys. Rev. Lett. 59, 1152 (1987).

[11] M. Przybylski and U. Gradmann, J. Phys. (Paris), Colloq. 49, C8 (1988).

[12] U. Gradmann, G. Liu, H. J. Elmers, and M. Przybylski, Hyperfine Interact. 57, 1845 (1990).

[13] H. J. Elmers, G. Liu, and U. Gradmann, Phys. Rev. Lett. 63, 566 (1989).

[14] W. Dürr et al., Phys. Rev. Lett. 62, 206 (1989).

[15] M. Albrecht, U. Gradmann, T. Reinert, and L. Fritsche, Solid State Commun. 78, 671 (1991).

[16] W. Weber et al., Phys. Rev. Lett. 65, 2058 (1990).

[17] R. Bergholz and U. Gradmann, J. Magn. Magn. Mater. 45, 389 (1984).

[18] M. Farle et al., Phys. Rev. B 47, 11 571 (1993).

[19] G. A. T. Allan, Phys. Rev. B 1, 352 (1970).

[20] C. Domb, J. Phys. A 6, 1296 (1973).

[21] E. Kneller, in Magnetism and Metallurgy, edited by A. E. Berkowitz and E. Kneller (Academic, London, 1969), Vol. 1, pp. 365–471.

[22] H. J. Elmers and U. Gradmann, Appl. Phys. A 51, 255 (1990).

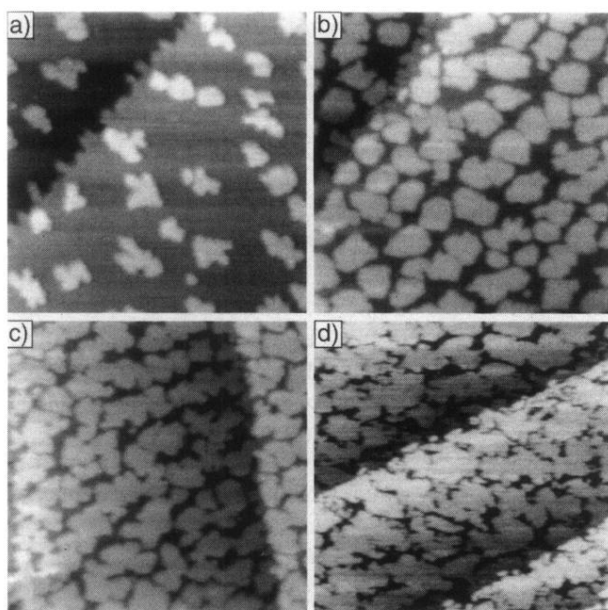FIG. 1. STM images of Fe(110) films, prepared at RT on W(110), all 70 nm × 70 nm in size, with [001] horizontal. (a) $\theta = 0.23$; (b) $\theta = 0.53$; (c) $\theta = 0.66$; (d) $\theta = 0.85$. Upper levels (Fe) bright; lower levels (W) dark.
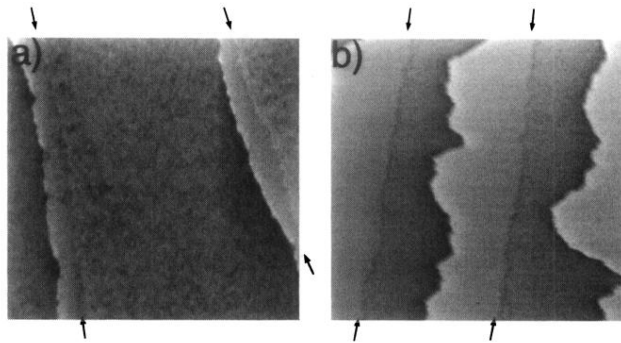
FIG. 3. As Fig. 1, but for films prepared at 570 K. (a) θ = 0.14; (b) θ = 0.52. The strong contrast marks the edge of the Fe layer; the faint contrast (straight line, indicated by arrows) the transition from W to Fe at the same level, at W steps.